Resonant excitation of high-order diocotron modes with rotating RF fields

M. Romé[1,2], G. Maero[1,2], N. Panzeri[1,2], R. Pozzoli[1]

[1] *Dipartimento di Fisica, Università degli Studi di Milano, Italy*

[2] *INFN Sezione di Milano, Italy*

An electron plasma can be confined for very long times in a Penning-Malmberg cylindrical trap. In a wide range of experimental parameters, the axially averaged electron plasma dynamics turns out to be analogous to that of a two-dimensional (2D) ideal (inviscid and incompressible) fluid with uniform density, the flow vorticity being proportional to the plasma density n and the stream function to the electrostatic potential ϕ [1]. Instabilities can arise in the system as a consequence of growing diocotron modes, i.e., density and potential perturbations with a spatial dependence of the form $\exp(il\theta)$, where the integer l represents the azimuthal wavenumber. The ability to excite and control low-frequency diocotron perturbations in a magnetized nonneutral plasma represents an opportunity to study dynamical properties of turbulent 2D fluids [2, 3, 4]. Recent investigations have directed attention to the behavior of strained flows under the action of externally imposed perturbations [5].

An electron plasma column with a monotonically decreasing radial density profile (or, ideally, a stepwise density profile), is stable against diocotron perturbations [6]. Under these conditions, diocotron waves are typically excited by means of suitable static or time-dependent multipolar drives applied on an azimuthally sectored electrode of the trap at the resonance frequency of the desired wavenumber. In general, this scheme is limited by the number N_s of electrically insulated azimuthal sectors of the electrode, yielding modes with $l \leq N_s/2$. Generalizing a previous work [7], it is demostrated both theoretically and experimentally that it is possible to overcome this limit and selectively excite high-order diocotron modes with applied electric fields which are co- or counter-rotating with respect to the azimuthal plasma rotation direction, by properly choosing the drive frequency and the phase difference between adjacent sectors. Assuming an ideal stepwise unperturbed radial density profile, $n_0(r) = n_0 H(R_P - r)$, where H denotes the Heaviside step function and R_P is the plasma radius, the equilibrium rotation frequency is given by $\omega_D = en_0/2\varepsilon_0 B$, where $-e$ is the electron charge, ε_0 the vacuum permittivity and B is the strength of the magnetic field (directed along the axial direction of the trap). The quantity ω_D is known as diocotron frequency, and sets the characteristic time scale of the $\mathbf{E} \times \mathbf{B}$ collective plasma modes. Here we refer explicitly to the application of sinusoidally time-varying potentials to a cylindrical electrode with $N_s = 8$ electrically insulated azimuthal sectors, but the results

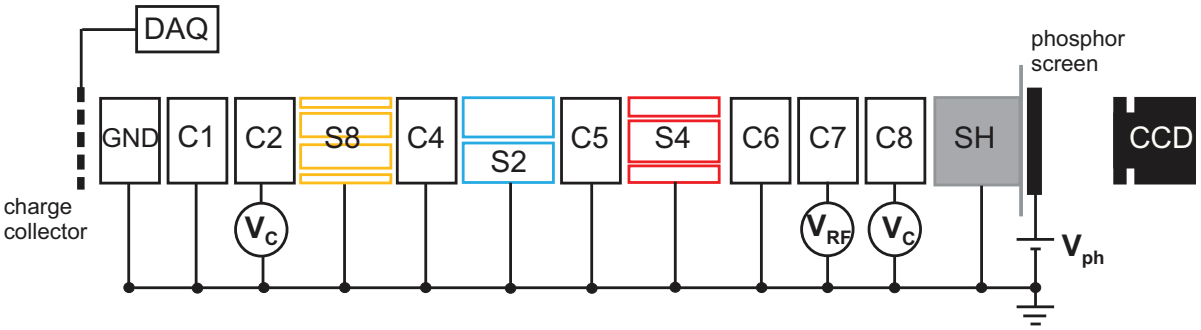

Figure 1: Sketch of the trap electrode arrangement. The outer electrodes GND and SH are permanently grounded. Two outer electrodes are used as endcaps (potential V_C) and an inner one for the plasma generation applying an oscillating voltage V_{RF}. The C's electrodes have a length of 9 cm. The S2, S4 and S8 electrodes are divided azimuthally into two, four and eight sectors, respectively, and have a length of 15 cm. Diagnostic tools are also sketched: A charge collector connected to a digital oscilloscope and a phosphor screen set to a potential $V_{ph} = 5 - 10$ kV, whose image is recorded by a CCD camera.

can be generalized to the case of an arbitrary number of sectors. The boundary potential reads

$$\delta\phi(r = R_W, \theta, t) = \sum_{m=0}^{7} V_m(t)[H(\theta - m\pi/4) - H(\theta - (m+1)\pi/4)], \tag{1}$$

where $V_m = V_d \cos(\omega_d t + \sigma m j \pi/4)$, with $\sigma = \pm 1$, and V_d and $\omega_d = 2\pi\nu_d$ the amplitude and angular frequency of the external drive, respectively. The cases $\sigma = -1$ and $\sigma = +1$ refer to "co-" and "counter-rotating" drives with respect to the azimuthal rotation of the unperturbed plasma, respectively (the magnetic field is assumed in the positive axial (z) direction, so that the electron plasma rotates in the positive azimuthal (θ) direction). The integer index j ranges from 1 to 4, corresponding to a phase difference between adjacent sectors of $\pi/4, \pi/2, 3\pi/4$ and π, respectively. The cases $j = 1, 2, 3$ correspond to rotating drives, while $j = 4$ is relevant to a non-rotating (octupole) drive. With the adopted phase relationship between the potentials on the eight azimuthal sectors, a Fourier analysis shows that the boundary potential can be written as a superposition of azimuthally propagating waves containing only modes of order $8k + j$ and $8(k+1) - j$, where k is an integer index. This fact suggests how to excite diocotron modes of (virtually) arbitrary order. Following Ref. [7], within the framework of a linear treatment a potential perturbation on the wall of the form $\delta\phi = \varepsilon \exp(il\theta - i\omega_d t)$, where ε denotes the amplitude, produces a potential perturbation on the plasma surface that is linearly growing with time,

$$\delta\phi(r = R_P, \theta, t) = \varepsilon \left(\frac{R_P}{R_W}\right)^l [1 + i(l\omega_D - \Omega_l)t] \exp(il\theta - i\Omega_l t), \tag{2}$$

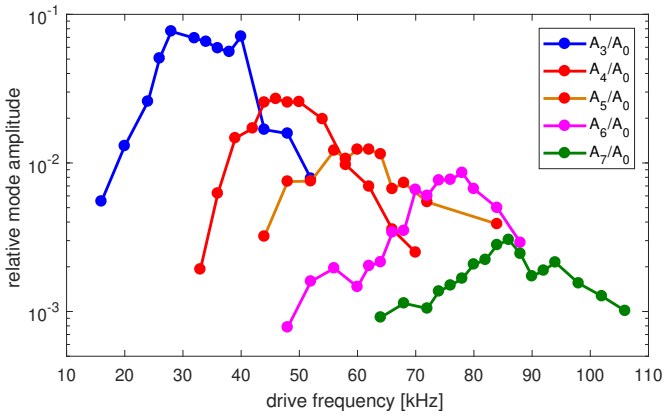

Figure 2: Amplitudes (normalized over A_0) of the dominant A_n Fourier modes of the plasma contour *vs* ν_d. The resonance curves are obtained with different excitation amplitudes and time spans: 1.7 V_{pp}, 200 ms ($l = 3$); 3.0 V_{pp}, 200 ms ($l = 4$); 2.5 V_{pp}, 100 ms ($l = 5$); 3.0 V_{pp}, 200 ms ($l = 6$); 3.4 V_{pp}, 100 ms ($l = 7$).

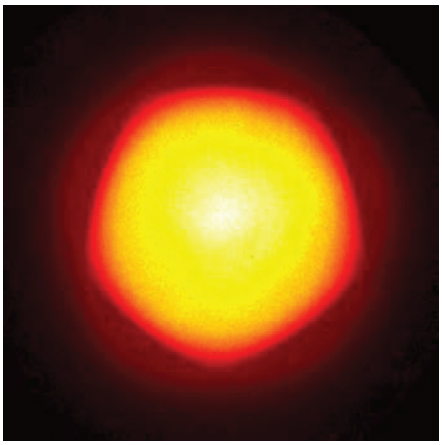

Figure 3: CCD image obtained with the application of a co-rotating drive with $V_d = 2.5$ V_{pp} and $\nu_d = 60$ kHz (corresponding to the maximum of the relevant resonance curve in Fig. 2).

and therefore a significant deformation of the plasma surface, only when $\omega_d = \Omega_l$, where $\Omega_l = \omega_D[l - 1 + (R_P/R_W)^{2l}]$ is the frequency of the l-th diocotron mode, and $l = 8k + j$ for $\sigma = -1$ or $l = 8(k+1) - j$ for $\sigma = 1$, respectively.

The experiments have been performed in the Penning-Malmberg trap ELTRAP [8]. A low density ($n \approx 1$–$2 \cdot 10^6$ cm^{-3}) electron plasma is contained within a stack of cylindrical electrodes (inner radius $R_W = 4.5$ cm), kept under ultra-high vacuum conditions (base pressure in the high 10^{-9} mbar range). A scheme of the trap is reported in Fig. 1. In the experiments reported here, the plasma is contained between C2 and C8 electrodes (the plug potential is $V_p = -80$ V) for a length $L_P \approx 90$ cm. The electron plasma is generated by applying a radio frequency (RF) drive [9] with amplitude $V_{RF} = 5.65$ V_{pp} and frequency 7.42 MHz to electrode C7 for 8–10 seconds. The generated plasma is characterized by an approximately flat radial density profile, with a mean square radius $\approx 0.5 R_W$. Just after the plasma generation drive is switched off, the diocotron excitation drive is applied to the S8 electrode. This drive is then switched off and at the same time the plasma is dumped against a positively biased ($V_{ph} = 8$ kV) phosphor screen grounding the electrode C8. The light emitted by the phosphor screen is collected by a charge coupled device (CCD) camera obtaining a snapshot of the axially averaged plasma density distribution. The magnetic field strength has been set at $B = 0.12$ T, while the frequency of the drive has been varied searching for resonances. In general, in the linear regime (low

amplitude drive, times of few plasma rotation periods) it is difficult to evaluate the effect of the perturbation potential directly from the CCD images. The reported results therefore refer to a mode excitation up to a fully developed nonlinear stage and long excitation times ($\geq$ 100 ms).

The deformation of the plasma cross section has been chosen as a measure of the mode excitation level. The contour of the plasma is determined as a sampled function $R_P(\theta)$ in the reference frame of the center of charge, detecting the crossing of a threshold level. The threshold is obtained as a θ-average of the values of the plasma density where its radial derivative (at any given θ) has maximum magnitude. The trigonometric Fourier expansion $R_P(\theta) = A_0/2 + \sum_{n=1}^{+\infty} A_n \sin(n\theta + \varphi_n)$ finally gives the amplitudes A_n of the sinusoidal azimuthal deformations of the contour. The experiments have been repeated at least 20 times for each drive frequency. The averaged Fourier mode amplitudes A_n (normalized over A_0, i.e., the corresponding mean plasma radius) *vs* the frequency ν_d of the applied drive is shown in Fig. 2. The resonance curves appear in general quite broad and the frequencies corresponding to their maxima are shifted with respect to the theoretical values obtained from the idealized case of a stepwise density profile. An example of plasma configuration obtained with the application of a co-rotating drive on the S8 electrode, showing a well defined pentagonal plasma cross-section is reported in Fig. 3. Preliminary measurements at resonance frequencies show that increasing V_d, a progressive decrease of the total plasma charge is observed. This effect is easily explained as the outermost part of the plasma column is lost to the radial wall in the interaction with the externally-imposed field. The possible role in the initial stage of the application of the diocotron excitation drive played by the population of positive ions produced during the RF plasma generation is presently under investigation. In conclusion, the experimental technique presented here has the potential to be efficiently used for the manipulation of a nonneutral plasma, allowing to selectively excite an arbitrary order diocotron mode by applying suitable co- or counter-rotating electric fields on azimuthally sectored electrodes.

References

[1] C.F. Driscoll and K.S. Fine, Phys. Fluids B **2**, 1359 (1990)

[2] M. Romé, S. Chen and G. Maero, Plasma Phys. Control. Fusion **59**, 014036 (2017)

[3] S. Chen, G. Maero and M. Romé, J. Plasma Phys. **83**, 705830303 (2017)

[4] M. Romé, S. Chen and G. Maero, AIP Conf. Proc. **1928**, 020012 (2018)

[5] N.C. Hurst, J.R. Danielson and C.M. Surko, J. Fluid Mech. **848**, 256 (2018)

[6] R.C. Davidson, *An Introduction to the Physics of Nonneutral Plasmas* (Addison-Wesley, 1990).

[7] G. Bettega, B. Paroli, R. Pozzoli and M. Romé, J. Appl. Phys. **105**, 053303 (2009)

[8] G. Maero, S. Chen, R. Pozzoli and M. Romé, J. Plasma Phys. **81**, 495810503 (2015)

[9] B. Paroli, F. De Luca, G. Maero, R. Pozzoli, and M. Romé, Plasma Sources Sci. Technol. **19**, 045013 (2010)